# SUPPORTING INFORMATION

# Assembly structures and electronic properties of truxene-porphyrin compounds studied by STM/STS

Haijun Xu, Hongyu Shi, Yuhong Liu, Jian Song, Xinchun Lu, Claude P. Gros, Ke Deng and Qingdao Zeng

**Table of contents**

# Experimental section

## Synthesis of ITIP, IT2P-1 and IT2P-2

The synthesis of **ITIP**, **IT2P-1** and **IT2P-2** is shown **in** Scheme 1. Compound **1a-b** and **2a-b** were synthesized according to the literature [1]. **3** was synthesized according to the literature [2]. Compounds **ITIP**, **IT2P-1** and **IT2P-2** were synthesized as previously described by us [1, 3].

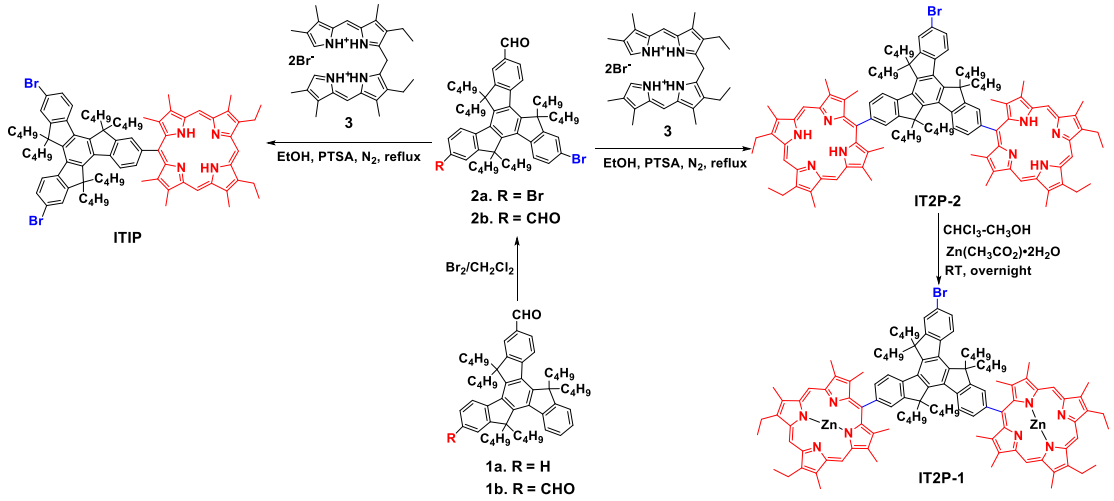


**Scheme S1.** Synthesis of **ITIP**, **IT2P-1** and **IT2P-2.**

## Synthesis of ITIP

A solution of 5,5',10,10',15,15'-hexabutyl-7, 12-dibromotruxene-2-carbaldehyde **2a** (865.0 mg, 1.0 mmol) and 1,19-dideoxy-8,12-diethyl-2,3,7,13,17,18- hexamethyl-a,c-biladien **3** (602.0 mg, 1.0 mmol) in ethanol (150 mL) was heated to reflux, and nitrogen was bubbled through the system. Then, 10.0 ml of a solution of para-toluene sulfonic acid (PTSA, 2.50 g) in ethanol was slowly added during 18 h. The deep red solution was refluxed for 48 h under $N_2$. The organic solvent was removed under reduced pressure. The residue was dissolved in $CH_2Cl_2$, washed with

saturated $NaHCO_3$ solution. The solvent was removed under vacuum and the remaining residue was purified by repeated column chromatography on silica gel with 60% $CH_2Cl_2$-heptane as eluents. The bright red band eluted was collected, dried, and under recrystalization from DCM/methanol. **ITIP** was obtained (Yield: 340.0 mg, 25%). $^1$H NMR ($CDCl_3$) δ (ppm): 10.21 (s, 2 H, meso-*H*), 9.99 (s, 1 H, meso-*H*), 8.73 (d, 1 H, J = 9.0 Hz, Ar-H), 8.29 (m, 3 H, Ar-*H*), 8.07 (d, 1 H, J = 6.0 Hz, Ar-H), 7.69-7.53 (m, 4 H, Ar-H), 4.10 (q, 4 H, pyrro-$CH_2CH_3$), 3.68 (s, 6 H, pyrro-$CH_3$), 3.56 (s, 6 H, pyrro-$CH_3$), 3.26 (m, 2 H, Truxene-$CH_2$-), 2.97 (m, 4 H, Truxene-$CH_2$-), 2.57 (s, 6 H, pyrro-$CH_3$), 2.20 (m, 6 H, -$CH_2$-), 1.91 (t, 6 H, J = 9.0 Hz, pyrro-$CH_2CH_3$), 1.09-0.98 (m, 12 H, -$CH_2$-), 0.85-0.56 (m, 30 H, -$CH_2$-$CH_3$). HR-MS (MALDI-TOF): m/z = 1282.6037 $[M]^+$, 1282.5996 calcd for $C_{81}H_{96}Br_2N_4$. UV/Vis ($CH_2Cl_2$):$\lambda_{max}$ (nm) (ε x $10^{-3}$ L $mol^{-1}$ $cm^{-1}$) = 285.0 (63.28), 301.9 (65.28), 314.0 (98.11), 404.0 (254.19), 503.0 (19.43), 537.0 (7.83), 571.0 (8.46), 625.0 (2.84), 653.9 (2.26).

**Synthesis of 1T2P-2**

A solution of 5,5',10,10',15,15'-hexabutyl-12-bromotruxene-2, 7-dicarbaldehyde **2b** (814.0 mg, 1.0 mmol) and 1,19-dideoxy-8,12-diethyl-2,3,7,13,17,18- hexamethyl-a,c-biladien **3** (1385.0 mg, 2.3 mmol) in ethanol (150 mL) was heated under reflux, and nitrogen was bubbled through the system. Then, 10.0 ml of a solution of para-toluene sulfonic acid (PTSA, 2.50 g) in ethanol was slowly added during 18 h. The deep red solution was refluxed for 48 h under $N_2$. The organic solvent was removed under reduced pressure. The residue was redissolved in 250 mL of $CH_2Cl_2$, washed with saturated $NaHCO_3$ solution. The organic solution was separated by use of a

separatory funnel and dried over $MgSO_4$. The solvent was removed under vacuum and the Zinc derivative was isolated by repeated column chromatography on silica gel with $CH_2Cl_2$ and $CHCl_3$ as eluents. The pure porphyrin compound was obtained as a purple solid after recrystallization from $CH_2Cl_2$/methanol. **1T2P-2** was obtained (Yield: 135 mg, 16%). $^1$H NMR ($CDCl_3$) δ (ppm): 10.24 (s, 2 H, meso-*H*), 10.21 (s, 2 H, meso-*H*), 10.01 (s, 1 H, meso-*H*), 9.99 (s, 1 H, meso-*H*), 8.76 (t, 2 H, J= 6 Hz, Ar-H), 8.40-8.29 (m, 3 H, Ar-*H*), 8.10 (d, 1 H, J = 6 Hz, Ar-H), 8. 04 (d, 1 H, J = 6 Hz, Ar-H), 7.74 (s, 1 H, Ar-H), 7.61 (m, 1 H, Ar-H), 4.10 (q, 8 H, pyrro-*CH*$_2$$CH_3$), 3.68 (s, 6 H, pyrro-*CH*$_3$), 3.66 (s, 6 H, pyrro-*CH*$_3$), 3.61 (s, 6 H, pyrro-*CH*$_3$), 3.58 (s, 6 H, pyrro-*CH*$_3$), 3.32 (m, 4 H, Truxene-*CH*$_2$-), 3.09 (m, 2 H, Truxene-*CH*$_2$-), 2.66 (s, 6 H, pyrro-$CH_3$), 2.62 (m, 6 H, pyrro-*CH*$_3$), 1.92 (m, 12 H, pyrro-$CH_2$*CH*$_3$), 1.29-1.18 (m, 12 H, -*CH*$_2$-), 0.85-0.74 (m, 30 H), -3.01 (s, 2 H, N-*H*), -3.19 (s, 2 H, N-H). MS (MALDI-TOF): m/z = 1653.71 $[M+H]^+$, 1653.17 calcd for $C_{111}H_{130}BrN_8^+$. HR-MS (MALDI-TOF): m/z = 1652.9634 $[M]^+$, 1652.9518 calcd for $C_{111}H_{129}BrN_8^+$. UV/Vis ($CH_2Cl_2$): $\lambda_{max}$ (nm) (ε x $10^{-3}$ L $mol^{-1}$ $cm^{-1}$) = 285.0 (61.79), 313.1 (86.56), 406.0 (530.03), 502.0 (41.50), 537.0 (17.15), 570.9 (18.95), 625.0(5.85).

**Synthesis of 1T2P-1**

2, 7-di(13, 17-diethyl-2, 3, 7, 8, 12, 18–hexamethylporphyrin-5-yl)- 12-bromo-5, 5', 10, 10', 15, 15'-hexabutyltruxene **9** (40 mg, 0.024 mmol) was dissolved in 40 mL of $CHCl_3$. $Zn(OAc)_2{\cdot}2H_2O$ (50 mg, ) in methanol (5 mL) was added. The reaction mixture was stirred overnight at room temperature. The solution was washed with water times and dried over $MgSO_4$. The product was

purified by column chromatography on silica gel with 60% DCM-heptane. **1T2P-1** was obtained **(**Yield: 42 mg, 98%). MS (MALDI-TOF): m/z = 1776.67 $[M]^+$, 1776.78 calcd for $C_{111}H_{125}BrN_8Zn_2^+$. HR-MS (MALDI-TOF): m/z = 1777.7844 $[M+H]^+$, 1777.7820 calcd for $C_{111}H_{126}BrN_8Zn_2^+$. UV/Vis ($CH_2Cl_2$): $\lambda_{max}$ (nm) ($\varepsilon$ x $10^{-3}$ L $mol^{-1}$ $cm^{-1}$) = 284.0 (66.78), 314.0 (86.56), 407.1 (740.02), 535.0 (39.87), 571.0 (31.35).

---

**Synthesis References**


[1] A. Langlois, H.-X. Xu, B. Brizet, F. Denat, J.-M. Barbe, C. P. Gros and P. D. Harvey, *J. Porphyrins Phthalocyanines - Special Issue* **2014**, *18*, 94-106. DOI: 110.1142/S1088424613501150.

[2] H.-J. Xu, B. Du, C. P. Gros, P. Richard, J.-M. Barbe and P. D. Harvey, *J. Porphyrins Phthalocyanines* **2013**, *17*, 44-55.

[3] A. Langlois, H.-J. Xu, P.-L. Karsenti, C. P. Gros and P. D. Harvey, *J. Porphyrins Phthalocyanines* **2015**, *Special Issue dedicated to Prof. Shunichi Fukuzumi*, 427-441.

**DFT-D3 method**

We have further performed DFT-D method to estimate the interaction energy between adsorbates and graphite, in which the London dispersion interaction in van der Waals interaction is included. In surface science, thousands of different systems including intermolecular and intramolecular cases have been investigated by DFT-D method successfully[S1]. Here, we employed DFT-D3 method based on the standard Kohn–Sham density functional theory. The corrected energy is added with an atom-pair wise (atom-triple wise) dispersion correction as follows[S2].

$$E_{DFT\text{-}D3} = E_{KS\text{-}DFT} + E_{disp} \quad (1)$$

In DFT-D3 method [33], the vdW-energy expression is:

$$E_{disp} = -\frac{1}{2}\sum_{i=1}^{Nat}\sum_{j=1}^{Nat}\sum_{L}{}'\left(f_{d,6}(r_{ij,L})\frac{C_{6ij}}{r_{ij,L}^{6}} + f_{d,8}(r_{ij,L})\frac{C_{8ij}}{r_{ij,L}^{8}}\right) \quad (2)$$

where $r_{ij,L}$ is the internuclear distance between atoms $i$ and $j$. The dispersion coefficients $C_{6ij}$ and $C_{8ij}$ are adjusted and depend on the local geometry around atoms $i$ and $j$. The Becke-Jonson (BJ) damping is used in the D3 method:

$$f_{d,n}(r_{ij}) = \frac{s_n r_{ij}^{n}}{r_{ij}^{n} + (a_1 R_{0ij} + a_2)^{n}} \quad (3)$$

where $R_{0ij} = \sqrt{\frac{C_{8ij}}{C_{6ij}}}$, the parameters $a_1$, $a_2$, $s_6$, and $s_8$ are adjustable depending on the choice of exchange-correlation functional.

**Benchmark to evaluate the accuracy of the DFT calculations**

To evaluate the accuracy of the DFT calculations, we have calculated the interaction between benzene and graphite, and the interaction between n-pentane and graphite as a benchmark. The

interaction between benzene and graphene is about -10.69 kcal·mol$^{-1}$, which agrees well with the experimental measurements (9.7～10 kcal·mol$^{-1}$ at T=298K[S3-S5]). The interaction between n-pentane and graphene is about -10.70 kcal·mol$^{-1}$, which is also in very good agreement with the theoretical formula (-10.15 kcal·mol$^{-1}$) for the energy of adsorption of n-alkanes on the surface of graphite was derived in previous papers[S6, S7] in this series: -Φ= 0.9 + 1.85 n kcal·mol$^{-1}$. It indicates that our results with DFT calculations are reasonable.

## Results

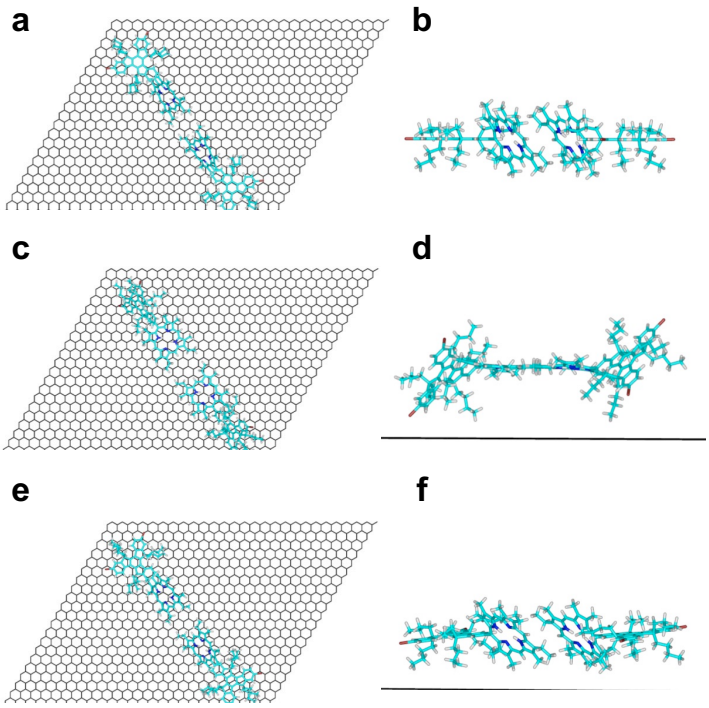


**Figure S1.** The calculated unit cell for **1T1P** adsorbed on graphene. (a) Top view and (b) side view for **1T1P-T flat** conformation. (c) Top view and (d) side view for **1T1P-P flat** conformation. (e) Top view and (f) side view for **1T1P-non flat** conformation.

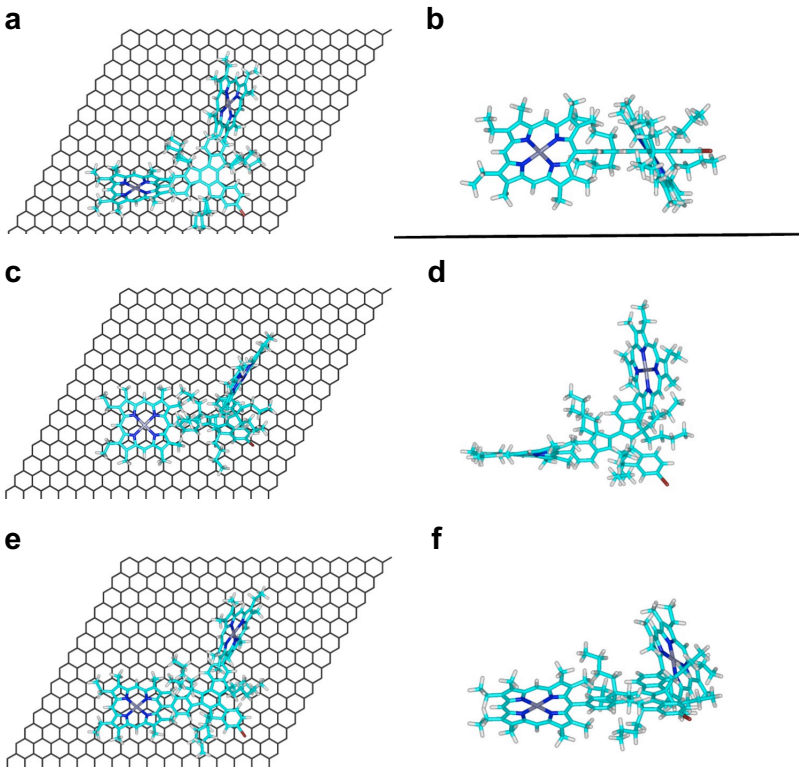


**Figure S2.** The calculated unit cell for **1T2P-1** adsorbed on graphene. (a) Top view and (b) side view for **1T2P-1-T flat** conformation. (c) Top view and (d) side view for **1T2P-1-P flat** conformation. (e) Top view and (f) side view for **1T2P-1-non flat** conformation.

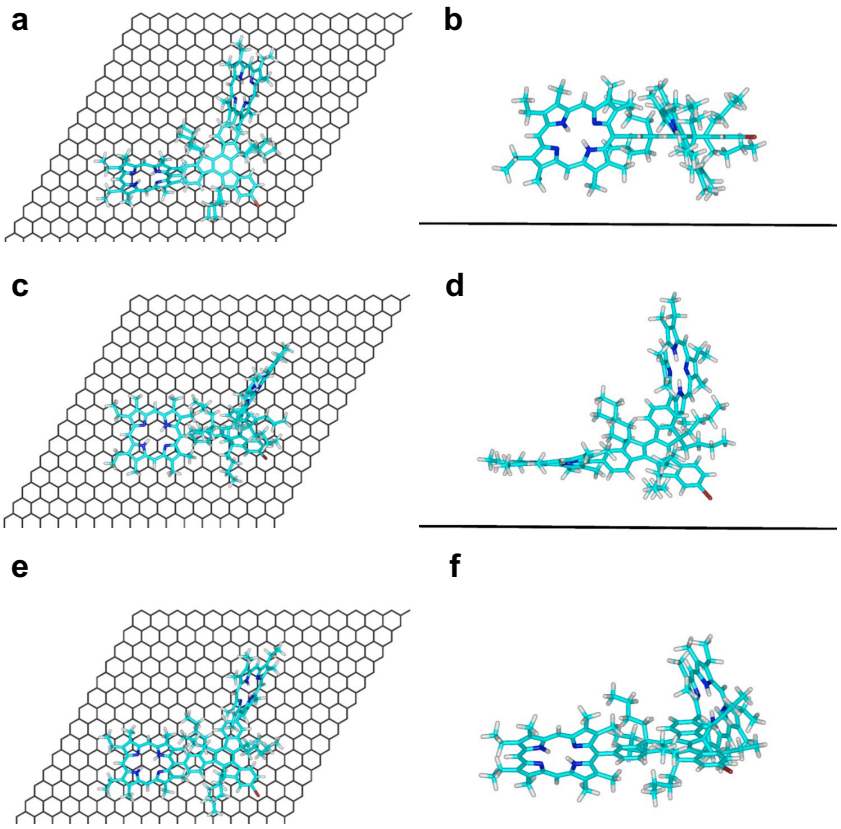


**Figure S3.** The calculated unit cell for **1T2P-2** adsorbed on graphene. (a) Top view and (b) side view for **1T2P-2-T flat** conformation. (c) Top view and (d) side view for **1T2P-2-P flat** conformation. (e) Top view and (f) side view for **1T2P-2-non flat** conformation.

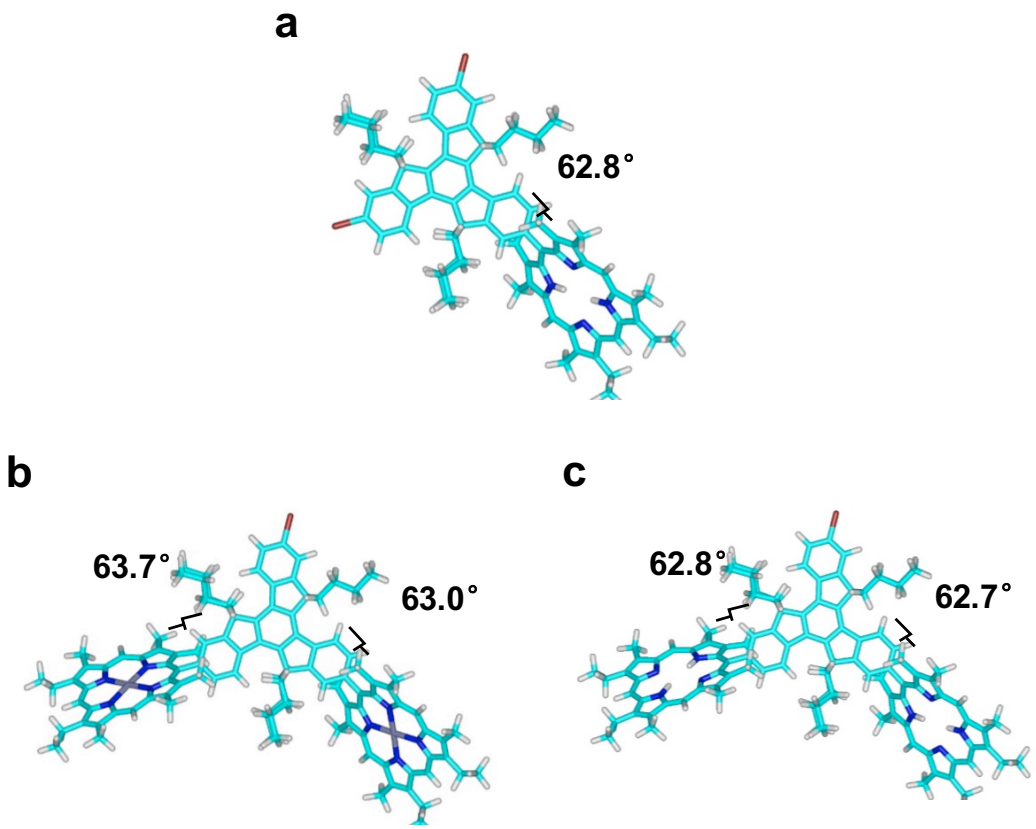


**Figure S4.** Illustrations for the torsion angles between the porphyrin unit and the truxene unit. (a) **1T1P**, (b) **1T2P-1**, (c) **1T2P-2**

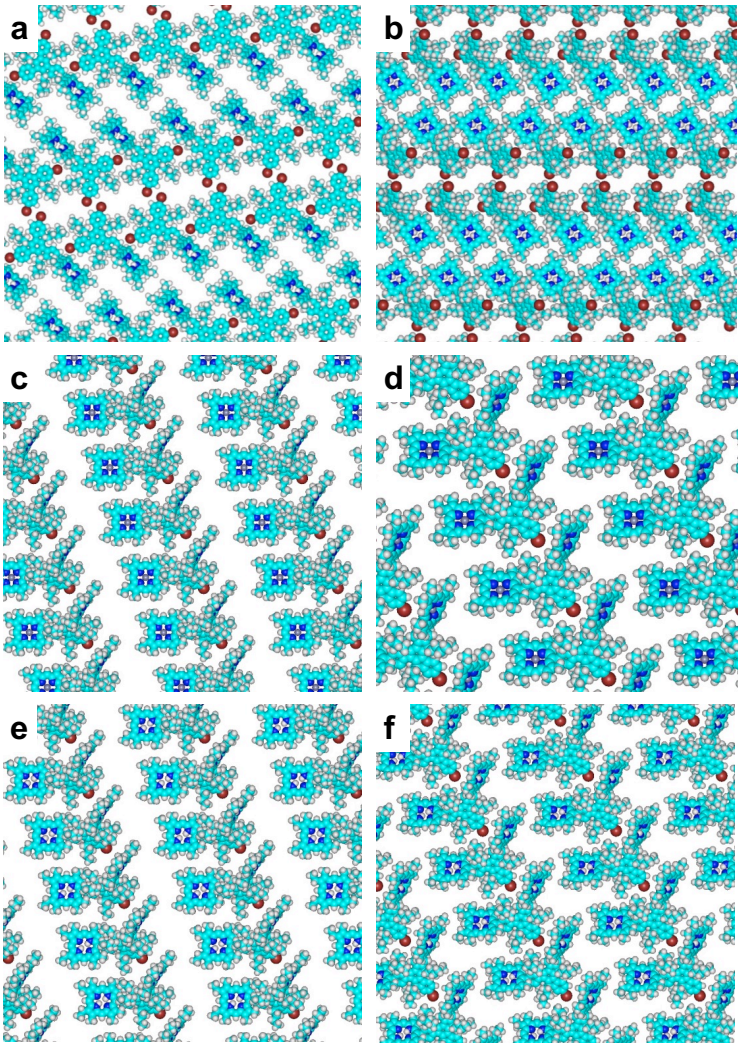


**Figure S5.** Optimized molecular models for the pristine assemblies. (a) **1T1P-T flat**, (b) **1T1P-P flat**, (c) **1T2P-1-P flat**, (d) **1T2P-1-non flat**, (e) **1T2P-2-P flat**, (f) **1T2P-2-non flat**

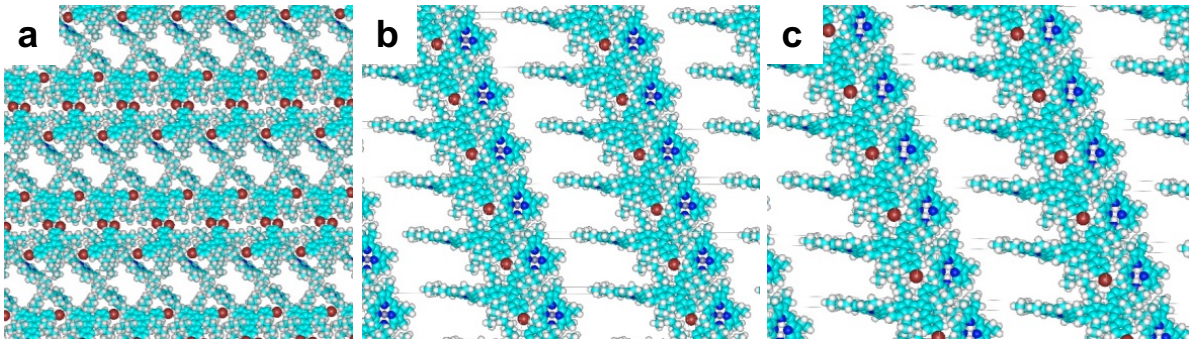


**Figure S6.** Side views of the optimized molecular models for the pristine assemblies. (a) **1T1P-non flat**, (b) **1T2P-1-T flat**, (c) **1T2P-2-T flat**.

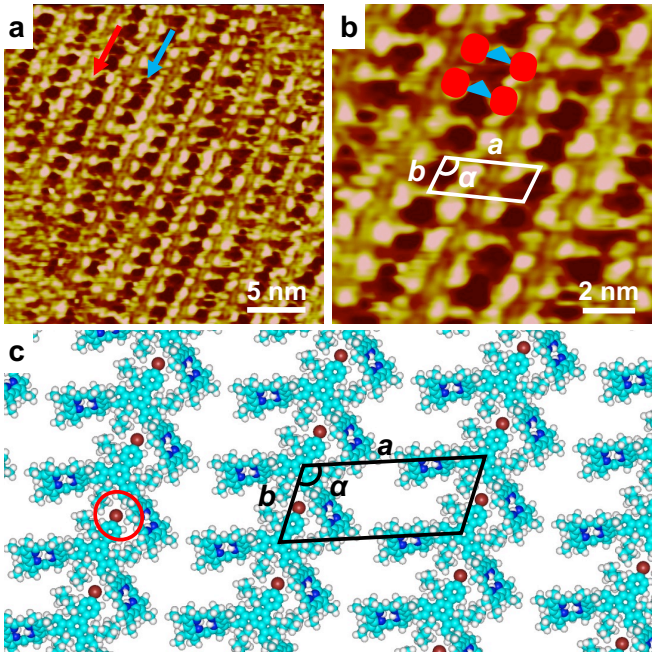


**Figure S7.** (a) Large-scale STM image of the pristine **1T2P-2** molecular assembly structure at the 1-phenyloctane/HOPG interface. The truxene and porphyrin units were pointed out by the blue and red arrows, respectively. (b) High-resolution STM image of **1T2P-2** assembly at the 1-phenyloctane/HOPG interface, superimposed with the colored schematic model to guide the eye. Tunneling conditions: $I_{set}$ = 198.4 pA, $V_{bias}$ = 935.4 mV. (c) Optimized molecular model for the pristine **1T2P-2** assembly.

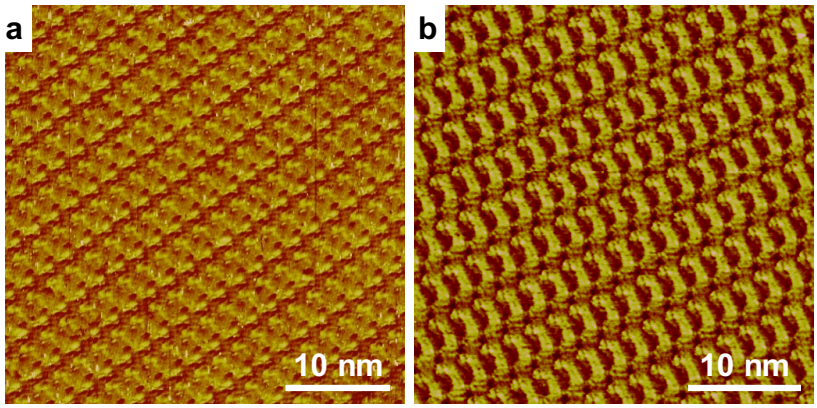


**Figure S8.** Large-scale STM images of (a) **TCDB** template and (b) **TCDB/1T1P** host-guest assembly at the 1-phenyloctane/HOPG interface. Tunneling conditions: (a) $I_{set}$ = 170.9 pA, $V_{bias}$ = 1020 mV; (b) $I_{set}$ = 189.2 pA, $V_{bias}$ = 1188 mV. The parameters of the unit cell overlaid on the STM image (**Figure 3a**) were measured as follows: $a_1$ = 3.9 ± 0.1 nm, $b_1$ = 2.2 ± 0.1 nm, $\alpha_1$ = 74 ± 1°, which coincide well with published results.[S8-S10]

**Table S1.** Total energies and energies per unit area for the different conformations for pristine **1T1P**, **1T2P-1** and **1T2P-2** assemblies on the HOPG surface with DFT-D3 method.

| | Interactions between adsorbates (kcal $mol^{-1}$) | Interactions between adsorbates and substrate (kcal $mol^{-1}$) | Total energy (kcal $mol^{-1}$) | Total energy per unit area (kcal $mol^{-1}$ $nm^{-2}$) |
|---|---|---|---|---|
| **1T1P-T flat** | -47.095 | -79.840 | -126.935 | -18.544 |
| **1T1P-P flat** | -31.708 | -37.319 | -69.027 | -10.084 |
| **1T1P-non flat** | -53.958 | -81.041 | -134.999 | -19.722 |
| **1T2P-1-T flat** | -25.282 | -54.494 | -79.776 | -15.872 |
| **1T2P-1-P flat** | -6.337 | -36.797 | -43.134 | -8.582 |
| **1T2P-1-non flat** | -6.974 | -22.309 | -29.283 | -5.826 |
| **1T2P-2-T flat** | -26.700 | -54.605 | -81.305 | -16.176 |
| **1T2P-2-P flat** | -6.16 | -35.303 | -41.463 | -8.249 |
| **1T2P-2-non flat** | -8.063 | -21.480 | -29.543 | -5.878 |

## DFT References


S1. S. Grimme, J.Antony, S. Ehrlich and H. Krieg, *J. Chem. Phys.*, 2010, **132**, 154104.

S2. J.P.B. Perdew, K. and M. Ernzerhof, *Phys. Rev. Lett.*, 1996, **77**, 3865.

S3. A. A. Isirikyan and A. V. Kiselev, *J. Phys. Chem.*, 1961, **65**, 601.

S4. R. A. Pierotti and R. E. Smallwood, *J. Colloid Interface Sci.*, 1966, **22**, 469.

S5. R. Zacharia, H. Ulbricht and T. Hertel, *Phys. Rev.B*, 2004, **69**, 155406.

S6. N. N. Avgul, G. I. Berezin, A. V. Kiselev, and I. A. Lygina. *L Phys. Chem.*, 1956, **30**, 2106.

S7. N. N. Avgul and A. V. Kiselev. *Proc. Acad. Sci. USSR*, 1957, **112**, 673.

S8. X. Zeng, S. Chang, K. Deng, J. Zhang, H. Sun, Q. Zeng and J. Xie, *Cryst. Growth Des.*, 2015, **15**, 3096-3100.

S9. X. Kong, K. Deng, Y. Yang, Q. Zeng and C. Wang, *J. Phys. Chem. C.*, 2007, **111**, 17382-17387.

S10. J. Xu, X. Xiao, K. Deng and Q. Zeng, *Nanoscale*, 2016, **8**, 1652-1657.